Applied Catalysis B: Environmental 127 (2012) 221–226

Contents lists available at SciVerse ScienceDirect

Applied Catalysis B: Environmental

journal homepage: www.elsevier.com/locate/apcatb

Electrochemical decomposition of urea with Ni-based catalysts

Wei Yan, Dan Wang, Gerardine G. Botte*

Center for Electrochemical Engineering Research, Chemical and Biomolecular Engineering Department, 165 Stocker Center, Ohio University, Athens, OH 45701, United States

ARTICLE INFO

Article history:
Received 16 April 2012
Received in revised form 16 July 2012
Accepted 23 August 2012
Available online 1 September 2012

Keywords:
Urea-rich wastewater
Environmental pollutants
Urea removal/decomposition
Ni-Zn and Ni-Zn-Co catalysts
Hydrogen production

ABSTRACT

Nickel based catalysts (Ni, Ni-Zn, and Ni-Zn-Co) synthesized through electrodeposition and alkaline leaching processes were used as electrocatalysts for the electrochemical decomposition of urea to benign nitrogen and fuel cell grade hydrogen. The performances of the Ni-based catalysts for the urea decomposition were investigated through cyclic voltammetry (CV) and polarization techniques. The results of the CVs show that the Ni-Zn catalysts and the Ni-Zn-Co catalysts decreased the onset potential of urea oxidation by 40 mV and 80 mV, respectively when compared to Ni catalysts. The highest efficiency for the oxidation of urea was observed with the Ni-Zn-Co catalysts. The Ni-Zn and Ni-Zn-Co catalysts are promising materials for large-scale urea removal/decomposition from urea-rich wastewater, as well as for hydrogen production.

1. Introduction

Fossil fuels, one of the important pillars of global economic development, are limited and non-renewable. The consumption of fossil fuels has caused environmental pollution and adverse climate change due to their high greenhouse gas emissions. To maintain the current energy consumption and to protect the global environment, it is imperative to seek and develop alternative energy sources. As the cleanest energy source, hydrogen is one of the most promising candidates for alternative energy sources [1–4]. However, challenges in developing the hydrogen economy include hydrogen production, storage, and transportation [5–7]. Suitable hydrogen carriers are required to meet certain standards, including: utilization efficiency, environmental compatibility, safety, and low cost. Urea ($CO(NH_2)_2$) has recently been considered as a hydrogen carrier for long-term sustainable energy supply due to its stable, relatively non-toxic, and non-flammable properties. Moreover, compared with gas/liquid hydrogen carriers, such as methanol, ethanol, and ammonia, urea is a solid substance at atmospheric pressure and temperature, which makes hydrogen storage and transportation considerably easier [8–10].

Urea is widely available throughout the world. Urea is synthesized on an industrial scale as a nitrogen-release fertilizer and animal feed additive. However, during the process of urea synthesis, a large amount of urea-rich wastewater is simultaneously produced [8–12]. In addition, urea is also the major constituent of human and animal urine, which results in large concentrations of urea in wastewater sewage systems [10,13]. For example, ~33 g of urea in urine is produced by an average adult per day [8]. The untreated urea-rich wastewater causes a detrimental effect on the environment, as it can go through a natural conversion to ammonia and then be emitted to the atmosphere. Ammonia in the atmosphere is unstable as it can be oxidized and therefore produce environmental pollutants, such as nitrites, nitrate, and nitric oxides. Once the rain washes out ammonia, nitric acid is formed. Ammonia poses dangers to the ground and drinking water, and causes health problems that cost billions of dollars [10,14–18]. Thus, management and treatment of urea have become important energy and environmental concerns.

Various methods, such as biological decomposition, chemical oxidation, and thermal hydrolysis, have been utilized for urea removal/decomposition [14,18–23]. However, these methods need sophisticated and bulky instruments, high temperature, and/or active enzyme (urease) for the biocatalytic decomposition of urea. Moreover, the immobilization, denaturation, and deactivation of the urease enzyme will limit the long term and large-scale decomposition of urea. Recently, electrochemical oxidation of urea from urea-rich wastewater has drawn increasing attention because (1) it is a well-controlled technique; (2) it can be operated for a long term, and it can be scaled up to large-scale manipulation processes of urea decomposition [10,12,14,15,24,25]. By applying a high current density on a platinized titanium electrode, Carlesi Jara et al. decreased the nitrate concentration of urea-rich wastewater [12]. Simka et al. successfully removed urea from the aqueous solutions using electrochemical treatment with Ti/Pt or Ti/(RuO_2–TiO_2) electrodes [14]. Inexpensive nickel was developed as a catalyst for urea

* Corresponding author. Tel.: +1 740 593 9670; fax: +1 740 593 0873.
E-mail address: botte@ohio.edu (G.G. Botte).

0926-3373/$ – see front matter © 2012 Elsevier B.V. All rights reserved.
http://dx.doi.org/10.1016/j.apcatb.2012.08.022

electrolysis that converted urea to hydrogen through electrochemical oxidation and accomplished the remediation of harmful nitrates in urea-rich wastewater [10]. The urea electrochemical oxidation process in alkaline media is described below:

$$CO(NH_2)_{2(aq)} + 6OH^- \rightarrow N_{2(g)} + 5H_2O_{(l)} + CO_{2(g)} + 6e^- \quad (1)$$

$$6H_2O_{(l)} + 6e^- \rightarrow 3H_{2(g)} + 6OH^-_{(aq)} \quad (2)$$

Reaction (1) occurs at the anodic compartment of the urea electrolyzer, while reaction (2) occurs at the cathodic compartment of the cell. The overall reaction is given by

$$CO(NH_2)_{2(aq)} + H_2O_{(l)} \rightarrow N_{2(g)} + 3H_{2(g)} + CO_{2(g)} \quad (3)$$

In order to reduce the overpotential and/or improve the oxidation current, Rh-Ni and Pt-Ir-Ni catalysts were studied as catalysts for urea electro-oxidation [24]. However, the requirements of noble metals (such as Pt, Ir, and Rh) increase the cost and limit the industrial scale applications for urea-rich wastewater treatments.

Recently, Ni-Co bimetallic hydroxide catalysts were prepared by incorporating cobalt into nickel hydroxide, which showed a significant reduction in the overpotential of urea electrooxidation compared to pure nickel catalysts [15]. However, the oxidation current density decreased with the addition of cobalt because cobalt has no electrocatalytic activity for urea oxidation. Therefore, efficient and inexpensive catalysts need to be synthesized to decrease the urea oxidation potential without the sacrifice of decreasing the oxidation current density in comparison to pure nickel catalysts. Within this context, this paper aims to synthesize Ni-based (Ni, Ni-Zn, Ni-Zn-Co) catalysts and determine the effects of the multimetal catalysts toward urea electrooxidation. The performances of the above different Ni-based catalysts for the urea electrooxidation were investigated and evaluated by means of cyclic voltammetry (CV) and polarization techniques.

2. Experimental

2.1. Chemicals and materials

Nickel (II) sulfate hexahydrate (98%), nickel (II) chloride hexahydrate (98%), zinc chloride (97%), cobalt (II) sulfate hexahydrate (98%), titanium wires (99.99%, 1.0 mm diameter), and titanium foils (99.99%, 0.127 mm thickness) were purchased from Alfa Aesar. Acetone (99+ %), propanol (99.5%), nitric acid (69.2%), sodium hydroxide (95+ %), potassium hydroxide (85.0+ %), and urea (99.7%) were obtained from Fisher Scientific. Boric acid (99+%) and ethanol (HPLC grade) were received from Acros Organics.

2.2. Electrode preparation

Titanium was chosen as the substrate material due to its reasonable cost and relatively strong corrosion resistance. In addition, titanium is not an active catalyst for the electrooxidation of urea; therefore, the effect of the deposited catalysts can be properly identified from this substrate. The electrode substrates were constructed by welding titanium wires to titanium foils using a SSW-2020att Miller resistance spot welder (1 s welder time, 90 Amps welding current, 50/60 Hz). Each titanium foil was coated with a teflon tape, except for a surface area of 1.5 cm × 1.0 cm. The surface conditions of the substrates were crucial to the adherent properties of electrodeposits. A rigorous pretreatment procedure was performed as follows. Firstly, titanium substrates were transferred into successive ultrasonic baths of soap, acetone, propanol and ultrapure water for 10 min each. Then, the substrates were immersed in 25 wt% sodium hydroxide and 18 wt% nitric acid for 5 min, respectively [26]. Before the samples were dried, they were rinsed in ultrapure water to remove any residual organics from the surface. After being dried, they were polished using 27.5 μm polishing alumina in a Crystal Mark, Inc. micro sandblaster for 30 s in order to provide a rough surface. Next, the substrates were again sonicated consecutively in acetone, propanol, and ultrapure water for 5 min each. Finally, the titanium foil substrates were completely dried in the oven at 80 °C.

The pure Ni, Ni-Zn bimetallic and Ni-Zn-Co trimetallic catalysts were electrodeposited on the pretreated titanium foil substrates with different preparation methods. The details of the bath composition, operation conditions, and procedure are summarized in Table 1. Both Ni and Co can be successfully electrodeposited at −0.85 V vs. Ag/AgCl based on our previous work [15]. However, Zn is more active than Ni and Co, and thus the deposition of Zn needs a more negative potential. As shown in the Fig. S4, the reduction potential of Zn (II) is around −1.6 V vs. Ag/AgCl. Therefore, the deposition potential of −1.6 V vs. Ag/AgCl was chosen as the 1st step for all metal electrodeposition and −0.85 V vs. Ag/AgCl was chosen for Co alone deposition in the 3rd step of the Ni–Zn–Co electrode. After preparing the Ni-based catalyst coatings, all catalyst/electrode samples were rinsed thoroughly with ultrapure water and dried in an oven at 80 °C overnight. A three-electrode electrochemical cell was employed during electrodeposition. It included a pretreated Ti foil as working electrode (1.5 cm × 1.0 cm), a platinum foil (4.0 cm × 4.0 cm) counter electrode, and a Ag/AgCl (saturated KCl solution) reference electrode. The reference electrode was positioned as close as possible to the surface of the working electrode through a Luggin capillary. The electrodeposition experiments were carried out at 35 °C using a Solartron 1470E potentiostat. During the deposition, the solution was stirred at 100 rpm with a 25.4 mm × 9.5 mm magnetic stirring bar. Electroplating processes of Ni and Ni–Zn were operated at a constant potential of −1.6 V vs. Ag/AgCl and the incorporation of cobalt into Ni–Zn bimetallic system was performed at a constant potential of −0.85 V vs. Ag/AgCl. The properties of the deposition films were affected by the applied voltage, current density, pH, bath composition, additives, and temperature [27]. It is necessary to note: (1) apart from being a pH buffer, boric acid can aid zinc deposition and promote nickel discharge [28,29]; (2) the addition of ethanol was to enhance the adhesion of precipitates to the substrate by changing the surface-tension characteristics of the precipitation process [30,31]; and (3) each catalyst/electrode sample (Ni, Ni-Zn after alkaline leaching of zinc, Ni-Zn-Co) had the same catalyst loading amount by strictly controlling the deposition time and temperature, which was finally ca. 1.9 mg cm^{-2}. Each electrode was cut into two parts (0.5 cm × 1.0 cm and 1.0 cm × 1.0 cm) for characterization and electrochemical testing.

2.3. Microscopic characterization

The morphological characteristics of the synthesized Ni alone, Ni-Zn bimetallic and Ni-Zn-Co trimetallic catalyst coatings were analyzed by scanning electron microscopy (SEM) using a JEOL-JSM-639OLV operated at 15 KV with magnifications of 3000 and 10,000. The chemical compositions of the synthesized Ni-based catalyst coatings were determined by energy dispersive X-ray (EDX) using a Genesis 2000- HX1622 attached to the SEM. The elemental mapping, equipped with EDX, was employed using 200 ms per pixel dwell time.

2.4. Electrochemical analysis

A typical three-electrode configuration cell was used for the electrochemical experiments. A Hg/HgO electrode equipped with a Luggin capillary and a platinum foil (4.0 cm × 4.0 cm) were chosen as the reference electrode and counter electrode, respectively. Before the electrochemical measurements, all electrode samples

Table 1
Experimental matrix for the synthesis of Ni-based catalyst coatings (Ni, Ni-Zn and Ni-Zn-Co).

Catalyst		Bath composition and procedure	Operation conditions
Ni	1st step	Electroplating in bath I: 33 g/L $NiSO_4.6H_2O$ + 4.5 g/L $NiCl_2.6H_2O$ + 3.7 g/L H_3BO_3 + 50:50 mixture (by volume) of ethanol and water	E = −1.6 V vs. Ag/AgCl T = 35 °C; t = 150 s
Leached Ni-Zn	1st step	Electroplating in Bath II: bath I + 8.6 g/L $ZnCl_2$	E = −1.6 V vs. Ag/AgCl; T = 35 °C; t = 300 s
	2nd step	Leaching of Zn in 30% NaOH	At 75 °C overnight
Leached Ni-Zn-Co	1st step	Electroplating in Bath II: bath I + 8.6 g/L $ZnCl_2$	E = −1.6 V vs. Ag/AgCl; T = 35 °C; t = 250 s
	2nd step	Leaching of Zn in 30% NaOH	At 75 °C overnight
	3rd step	Electroplating in bath III: 3.7 g/L $CoSO_4.6H_2O$ + 3.7 g/L H_3BO_3 + 50:50 mixture (by volume) of ethanol and water	E = −0.85 V vs. Ag/AgCl; T = 35 °C; t = 300 s

E means the deposition potential; T stands for the temperature of deposition; t indicates the deposition time.

were activated by 40 cycles of cyclic voltammetry from −0.1 V to 0.65 V vs. Hg/HgO at 20 mVs^{-1} in 5M KOH solution. The electrochemical activities of the Ni-based catalysts/electrodes were examined in 5M KOH solution in the absence and presence of 0.33M urea by cyclic voltammetry and chronoamperometric techniques using a Solartron 1470E potentiostat. The concentration of 0.33M urea was used during the experiment to simulate the concentration of urea in urine waste. The cyclic voltammograms experiments (CVs) were performed between −0.1 V and 0.65 V vs. Hg/HgO at a scan rate of 10 mVs^{-1}. In all the cases the sustained periodic state was achieved after 10 sweeps. The chronoamperometry experiments were performed at a constant potential of 0.52 V vs. Hg/HgO for 12 h.

The voltage step experiments were operated in 5M KOH solution both in the absence and presence of 0.33M urea at room temperature; the experiments were controlled using an Arbin instrument's potentiostat BT-2000. Electrodes of Ni alone, Ni–Zn and Ni–Zn–Co (1.0 cm × 1.0 cm) were chosen as anodes, respectively, and a platinum foil (4.0 cm × 4.0 cm) as cathode. The cell voltage was stepped from 1.35 to 1.60 V in 25 mV increments with a 30 s step time and stirred at 60 rpm.

3. Results and discussion

3.1. SEM and EDX analysis

The SEM images of Ni alone, the non-leached Ni-Zn (before alkaline leaching of zinc), the leached Ni-Zn (after alkaline leaching of zinc), and Ni-Zn-Co catalyst coatings are shown in Fig. 1. The Ni alone and the non-leached Ni-Zn coatings show dense morphologies with little or no cracks (Fig. 1a and b and Fig. S1a and b). However, the microstructure of the Ni-Zn coating undergoes significant changes after alkaline leaching of Zn. As shown in Fig. 1c, several cracks are presented on the surfaces of the Ni-Zn coating as a

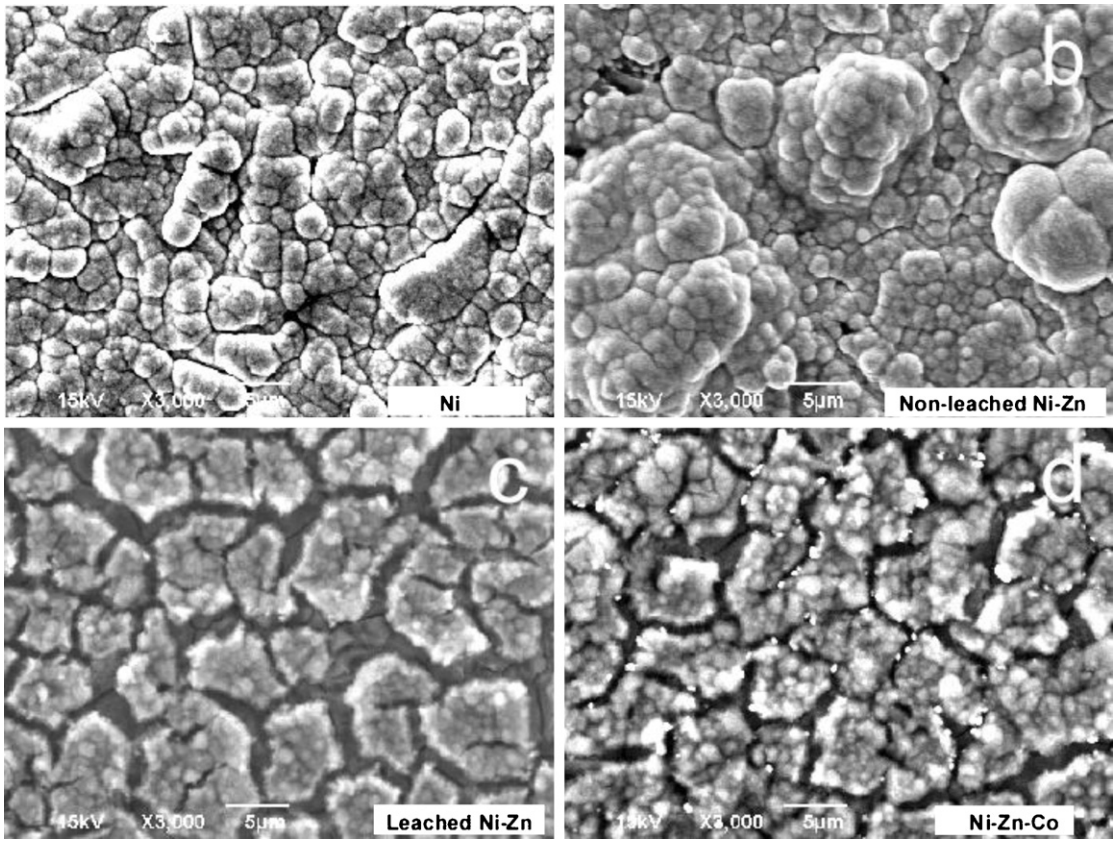

Fig. 1. SEM images of Ni-based catalysts with a magnification of 3000. (a) Ni alone, (b) non-leached Ni-Zn, (c) leached Ni-Zn, (d) Ni-Zn-Co. The images reveal that cracked and rough surface structures are formed on the Ni-Zn and Ni-Zn-Co catalysts as a result of the alkaline leaching of zinc.

Table 2
Chemical composition of the different catalysts according to EDX (Ni, Ni-Zn before alkaline leaching, Ni-Zn after alkaline leaching, and Ni-Zn-Co). All values are reported in atomic (at) %.

Catalyst	Element		
	Ni	Zn	Co
Ni	100.0	0	0
Ni-Zn before alkaline leaching of zinc	17.5 ± 0.3	82.5 ± 0.3	0
Ni-Zn after alkaline leaching of zinc	62.4 ± 0.2	37.6 ± 0.2	0
Ni-Zn-Co	51.0 ± 0.4	30.3 ± 0.4	18.7 ± 0.4

result of the leaching of zinc. The higher magnification SEM images of Ni-Zn catalyst coatings further show the relatively smooth surface changed to rough net-like structure after leaching of zinc (Fig. S1c). The formation of numerous cracks and rough surface leads to the increase of catalytic surface areas, which is helpful in improving their electrocatalytic activities for urea oxidation. For the Ni–Zn–Co electrodes, Ni and Zn were firstly electrodeposited on Ti substrates. Then the Ni–Zn coated electrodes were immersed in NaOH solution for the leaching of Zn and the formation of the cracked surfaces. Finally Co was deposited on the leached Ni–Zn electrodes. The cracked surfaces remain when cobalt is further deposited on the leached Ni-Zn coating (Fig. 1d and Fig. S1d). Elemental mapping results of Ni-Zn-Co trimetallic catalysts are displayed in Fig. S2 as well as the cross-section view in Fig. S3. Because there are lots of cracks in the electrodes after Zn leaching (Fig. 1c and d), the Co were not only deposited as a layer on the top surface of Ni-Zn, but also deposited into the cracks. The chemical compositions of all Ni-based catalysts are shown in Table 2. The chemical composition of the non-leached Ni-Zn coating is ca. 17.5 at% Ni and 82.5 at% Zn. After the alkaline leaching, the Zn content in the Ni–Zn alloy system dramatically decreases to 37.6 at%. This confirms that the dissolution of Zn leads to the formation of cracked surfaces on Ni-Zn and Ni-Zn-Co catalysts.

3.2. Cyclic voltammetry performance

The cyclic voltammetry results of the Ni alone, Ni-Zn after leaching of zinc, and Ni-Zn-Co catalysts/electrodes for urea electrooxidation are presented in Fig. 2. Fig. 2a shows a comparison of the CVs using pure Ni electrode in 5M KOH in the absence and presence of 0.33M urea. A pair of redox peaks is shown in the 5M KOH solution at a scan rate 10 mvs^{-1} due to the reversible transformation between NiOOH and $Ni(OH)_2$. In the presence of urea solution, the Ni electrode exhibits a relatively high anodic current with ca. 22 mA cm^{-2} peak current density and ca. 0.43 V (vs. Hg/HgO) onset potential of urea oxidation. Fig. 2b shows the urea electrooxidation performances on the leached Ni–Zn electrode. The onset potential of urea oxidation is negatively shifted to ca. 0.39 V vs. Hg/HgO and the oxidation peak current is increased to ca. 67 mA cm^{-2}. The leaching of zinc in alkaline solution increases catalytic surface area, exposes more active sites for urea oxidation, and thus results in a decrease of overpotential and the increase of oxidation current. The electroactive surface areas (ESA) of Ni and the leached Ni-Zn were further calculated according to the following equation [32–35]:

$$\mathrm{ESA} = \frac{Q}{(m\,q)} \tag{4}$$

where Q is the charge required to reduce NiOOH to $Ni(OH)_2$, which can be calculated from the cyclic voltammograms (curve 1 in Fig. 2 a, and b), m is the loading amount of the nickel catalysts and q is the charge associated with the formation of a monolayer of $Ni(OH)_2$. The q is 257 μC cm^{-2} as only one electron is needed from NiOOH to $Ni(OH)_2$ [36–38]. The electroactive surface areas

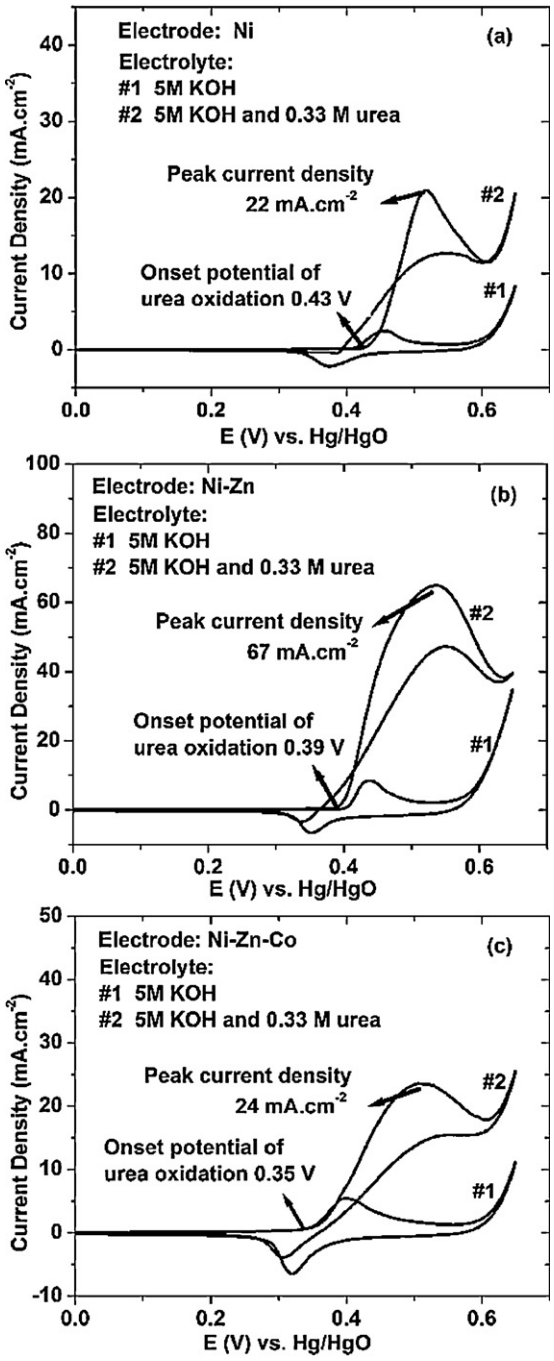

Fig. 2. Cyclic voltammetry of Ni-based catalysts in 5M KOH solution in the absence (#1) and presence (#2) of 0.33M urea at a scan rate of 10 mVs^{-1}. (a) Ni alone, (b) Ni-Zn, (c) Ni-Zn-Co. The CVs of the Ni-Zn electrodes show that the oxidation peak current is three times higher than the Ni alone catalyst, while the onset oxidation potential is reduced by ca. 40 mV. The Ni-Zn-Co catalysts decrease the onset oxidation potential by ca. 80 mV with respect to the Ni alone, while maintaining similar oxidation current densities.

of Ni and the leached Ni-Zn are calculated as 12.1 cm^2 mg^{-1} and 67.9 cm^2 mg^{-1}, respectively.

By further incorporating the Co into the Ni–Zn alloy system, the Ni–Zn–Co electrode shows ca. 0.35 V (vs. Hg/HgO) onset potential of urea oxidation (Fig. 2c). Compared to the pure Ni electrode (Fig. 2a), a total ca. 80 mV decrease in the onset potential of urea oxidation is achieved, since cobalt can promote the nickel to reach a higher oxidation state and facilitate the electron transfer of

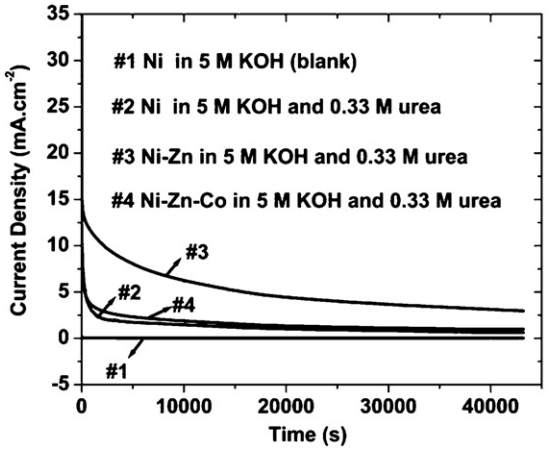

Fig. 3. Chronoamperograms of Ni-based catalysts in 5M KOH and 0.33M urea solution. Applied potential was 0.52 V vs. Hg/HgO. The curves reveal that all Ni-based multi-metal catalysts are stable and active for urea oxidation in alkaline solution, although the current slowly decreases over time due to the urea consumption from the solution.

urea oxidation [15,39]. The Ni–Zn–Co electrode also exhibits ca. 24 mA cm^{-2} peak current density and ca. 0.50 V (vs. Hg/HgO) peak potential of urea oxidation, which is similar with that of the pure Ni electrode. Therefore, unlike Ni–Co electrode [15,39], Ni–Zn–Co electrode decreases the onset potential of urea oxidation without the sacrifice of decreasing the oxidation current density compared to the pure Ni electrode.

3.3. Chronoamperometry comparison

Chronoamperometric experiments were used to further evaluate the electrocatalytic activities of Ni alone, the leached Ni-Zn, and Ni-Zn-Co catalysts/electrodes for urea oxidation. The experiments took place at a constant voltage of 0.52 V vs. Hg/HgO, which is the peak potential of urea oxidation on the Ni alone electrode (Fig. 2a). As shown in Fig. 3, a higher current density is produced on all electrodes (Ni, Ni–Zn, Ni–Zn–Co) in the presence of urea than that in the absence of urea electrolyte. The chronoamperometric results indicate that all Ni-based multi-metal catalysts are active and stable for urea oxidation, although the current slowly decreases over time due to the urea consumption from the solution. Compared to the Ni alone, the Ni-Zn catalyst shows the highest current density for the oxidation of urea and the Ni-Zn-Co catalyst keeps a similar current density as Ni alone, which agrees well with the results of the CVs.

3.4. Voltage step measurements

Voltage step analyses of Ni alone, the leached Ni-Zn, and Ni-Zn-Co catalysts/electrodes versus a cathode of Pt foil are shown in Fig. 4. The voltage step experiments aim to quantify the amount of current generated from urea electrolysis and water electrolysis at different cell voltages. The efficiency of urea electrolysis on Ni-based catalysts/electrodes can be evaluated by analyzing the percentage of

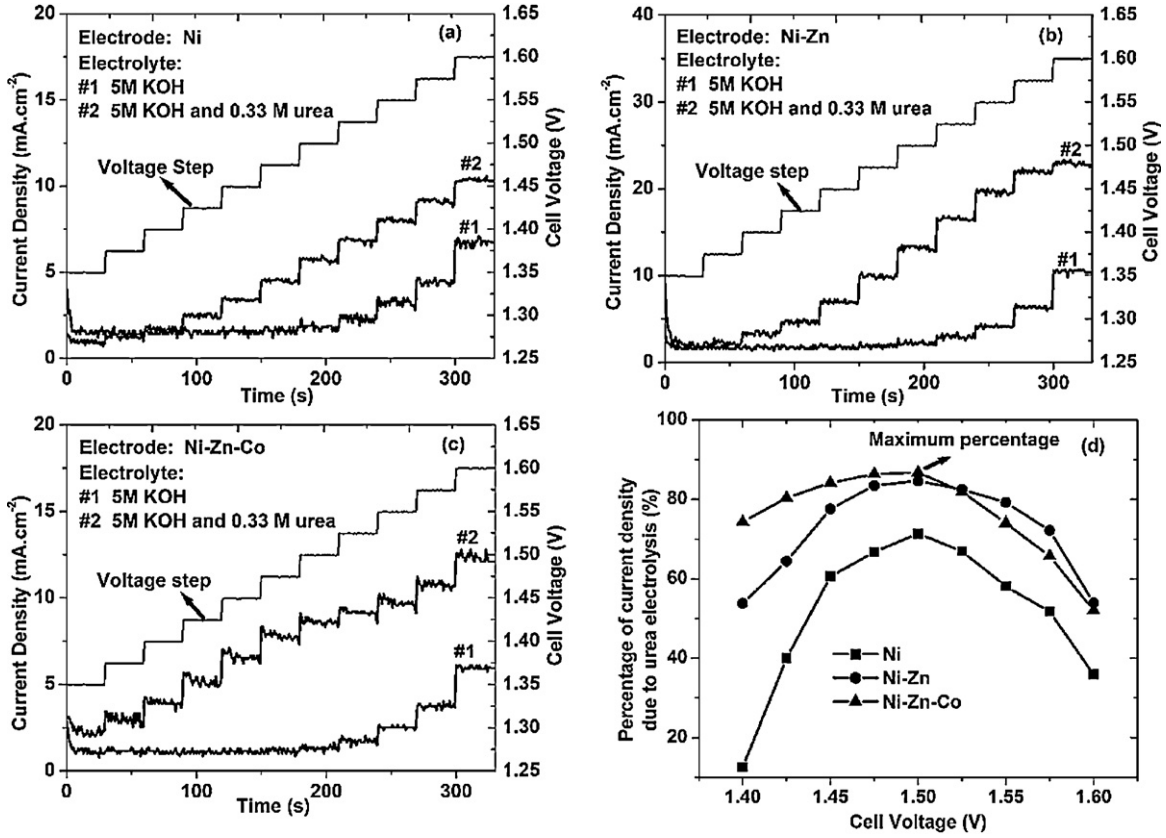

Fig. 4. Current density at different cell voltages on all Ni-based catalysts. (a) Ni alone, (b) Ni-Zn, (c) Ni-Zn-Co, (d) percentage of current density due to urea electrolysis at different cell voltage on Ni-based electrodes. Cell voltage was stepped from 1.35 to 1.60 V with Ni, Ni-Zn or Ni-Zn-Co each as the anode and with a platinum foil cathode in 1 M KOH solution in the absence (#1) and the presence (#2) of 0.33M urea. The results exhibit that Faradaic efficiency of urea electrolysis is improved by the incorporation of zinc and cobalt into the nickel system.

current density due to urea electrolysis. The percentages of current density due to urea electrolysis on Ni-based electrodes are shown in Fig. 4d. The maximum current portion attributed to urea electrolysis on Ni alone, Ni–Zn, and Ni–Zn–Co electrodes are ca. 71%, 83% and 87%, respectively, when cell voltage is 1.50 V. Moreover, the Ni-Zn and Ni-Zn-Co catalysts keep higher efficiency in the whole range of cell voltages than Ni alone. Compared with the other two, the advantage of the Ni–Zn–Co electrode becomes even more evident when the cell voltage is less than 1.50 V. For example, when cell voltage reaches 1.40 V, ca.74% of total current density is from urea electrolysis on the Ni–Zn–Co electrode and only ca. 12% of total current density on Ni alone as well as ca. 54% on the Ni–Zn electrode. The reason why Ni–Zn–Co trimetallic electrodes contribute to the high efficiency of urea electrolysis at low cell voltage is that cobalt can inhibit water electrolysis by increasing the overpotential of the oxygen evolution reaction [15,31,39] thereby promoting urea electrolysis. Therefore, the voltage step experiments exhibit that Faradaic efficiency of urea electrolysis is improved by the incorporation of zinc and cobalt into the nickel system. Faradaic efficiency of urea electrolysis decreases on all Ni-based electrodes when the cell voltage surpasses 1.50 V due to the completely developed water electrolysis.

4. Conclusion

Ni alone, Ni-Zn and Ni-Zn-Co catalysts were prepared through electrodeposition and alkaline leaching processes. The morphologies and chemical compositions of the catalysts were investigated by scanning electron microscopy and energy dispersive X-ray. The CVs of the Ni–Zn electrodes show that the oxidation peak current is three times as high and the onset oxidation potential is reduced by ca. 40 mV compared to the Ni alone catalysts. The Ni-Zn-Co catalysts decreased the onset oxidation potential of total ca. 80 mV and maintained similar oxidation current as Ni alone catalysts. Higher Faradaic efficiency towards urea electrolysis is observed by incorporating zinc and cobalt in to the nickel catalyst system. Therefore, the Ni-Zn and Ni-Zn-Co electrocatalysts are promising materials for the scale-up of the urea electrolysis technology and its application on the urea removal from urea-rich wastewater, as well as for hydrogen production.

Acknowledgments

The authors would like to thank the financial support of the Center for Electrochemical Engineering Research at Ohio University, and the Department of Defense through the U.S. Army Construction Engineering Research Laboratory (W9132T-09-1-0001). The content of the information does not reflect the position or the policy of the U.S. government.

Appendix A. Supplementary data

Supplementary data associated with this article can be found, in the online version, at http://dx.doi.org/10.1016/j.apcatb.2012.08.022.

References

[1] K. Faungnawakij, Y. Tanaka, N. Shimoda, T. Fukunaga, R. Kikuchi, K. Eguchi, Applied Catalysis B: Environmental 74 (2007) 144–151.
[2] C. Wu, L. Wang, P.T. Williams, J. Shi, J. Huang, Applied Catalysis B: Environmental 108–109 (2011) 6–13.
[3] R. Solmaz, A. Doener, G. Kardas, International Journal of Hydrogen Energy 34 (2009) 2089–2094.
[4] R. Muangrat, J.A. Onwudili, P.T. Williams, Applied Catalysis B: Environmental 100 (2010) 143–156.
[5] R.R. Davda, J.W. Shabaker, G.W. Huber, R.D. Cortright, J.A. Dumesic, Applied Catalysis B: Environmental 56 (2005) 171–186.
[6] V. Tozzini, V. Pellegrini, Journal of Physical Chemistry C 115 (2011) 25523–25528.
[7] L. Schlapbach, A. Zuettel, Nature 414 (2001) 353–358.
[8] A.N. Rollinson, J. Jones, V. Dupont, M.V. Twigg, Energy and Environmental Science 4 (2011) 1216–1224.
[9] A.N. Rollinson, G.L. Rickett, A. Lea-Langton, V. Dupont, M.V. Twigg, Applied Catalysis B: Environmental 106 (2011) 304–315.
[10] B.K. Boggs, R.L. King, G.G. Botte, Chemical Communications (32) (2009) 4859–4861.
[11] D. Wang, W. Yan, G.G. Botte, Electrochemistry Communications 13 (2011) 1135–1138.
[12] C. Carlesi Jara, S. Giulio, D. Fino, P. Spinelli, Journal of Applied Electrochemistry 38 (2008) 915–922.
[13] S. Kojima, A. Bohner, N. von Wiren, The Journal of Membrane Biology 212 (2006) 83–91.
[14] W. Simka, J. Piotrowski, A. Robak, G. Nawrat, Journal of Applied Electrochemistry 39 (2009) 1137–1143.
[15] W. Yan, D. Wang, G.G. Botte, Electrochimica Acta 61 (2012) 25–30.
[16] M.R. Rahimpour, H.R. Mottaghi, M.M. Barmaki, Fuel Processing Technology 91 (2010) 600–612.
[17] R.L. King, G.G. Botte, Journal of Power Sources 196 (2011) 2773–2778.
[18] W. Simka, J. Piotrowski, G. Nawrat, Electrochimica Acta 52 (2007) 5696–5703.
[19] G. Estiu, K.M. Merz Jr., Journal of the American Chemical Society 126 (2004) 11832–11842.
[20] D. Suarez, N. Diaz, K.M. Merz Jr., Journal of the American Chemical Society 125 (2003) 15324–15337.
[21] M.R. Rahimpour, Chemical Engineering and Processing 43 (2004) 1299–1307.
[22] V. Magne, M. Amounas, C. Innocent, E. Dejean, P. Seta, Desalination 144 (2002) 163–166.
[23] S.K. Gupta, R. Sharma, Water Research 30 (1996) 593–600.
[24] R.L. King, G.G. Botte, Journal of Power Sources 196 (2011) 9579–9584.
[25] D.A. Daramola, D. Singh, G.G. Botte, Journal of Physical Chemistry A 114 (2010) 11513–11521.
[26] I. Herraiz-Cardona, E. Ortega, V. Perez-Herranz, Electrochimica Acta 56 (2011) 1308–1315.
[27] N. Eliaz, K. Venkatakrishna, A.C. Hegde, Surface and Coatings Technology 205 (2010) 1969–1978.
[28] C. Karwas, T. Hepel, Journal of the Electrochemical Society 136 (1989) 1672–1678.
[29] J.P. Hoare, Journal of the Electrochemical Society 134 (1987) 3102–3103.
[30] K.P. Ta, J. Newman, Journal of the Electrochemical Society 145 (1998) 3860–3874.
[31] J.-W. Kim, S.-M. Park, Journal of the Electrochemical Society 150 (2003) E560–E566.
[32] B.Y. Xia, J.N. Wang, X.X. Wang, Journal of Physical Chemistry C 113 (2009) 18115–18120.
[33] E.P. Lee, Z. Peng, D.M. Cate, H. Yang, C.T. Campbell, Y. Xia, Journal of the American Chemical Society 129 (2007) 10634–10635.
[34] C.A. Li, K.N. Han, M.-P.N. Bui, X.-H. Pham, M.H. Hong, M. Irfan, Y.S. Kim, G.H. Seong, Journal of Applied Electrochemistry 41 (2011) 1425–1431.
[35] D. Wang, W. Yan, S.H. Vijapur, G.G. Botte, Journal of Power Sources 217 (2012) 498–502.
[36] S.A.S. Machado, L.A. Avaca, Electrochimica Acta 39 (1994) 1385–1391.
[37] I.J. Brown, S. Sotiropoulos, Journal of Applied Electrochemistry 30 (2000) 107–111.
[38] F. Hahn, B. Beden, M.J. Croissant, C. Lamy, Electrochimica Acta 31 (1986) 335–342.
[39] M. Vidotti, M.R. Silva, R.P. Salvador, S.I. Cordoba de Torresi, L.H. Dall'Antonia, Electrochimica Acta 53 (2008) 4030–4034.